SUPPORTING INFORMATION

Nanocomposite Scaffolds for Monitoring of Drug Diffusion in Three-Dimensional Cell Environments by Surface-Enhanced Raman Spectroscopy

Javier Plou,[1,2,3,#] Beatriz Molina-Martínez,[1,#] Clara García-Astrain,[1,2] Judith Langer,[1,2] Isabel García,[1,2] Amaia Ercilla,[3,4] Govindaraj Perumal,[1] Arkaitz Carracedo,[3,4,5,6] Luis M. Liz-Marzán*[,1,2,5]

[1] CIC biomaGUNE, Basque Research and Technology Alliance (BRTA), 20014 Donostia-San Sebastián, Spain.

[2] Biomedical Research Networking Center in Bioengineering, Biomaterials, and Nanomedicine (CIBER-BBN), 20014 Donostia-San Sebastián, Spain.

[3] CIC bioGUNE, Basque Research and Technology Alliance (BRTA), 48160 Derio, Spain.

[4] Biomedical Research Networking Center in Cancer (CIBERONC), 48160, Derio, Spain.

[5] IKERBASQUE, Basque Foundation for Science, 48009 Bilbao, Spain.

[6] Biochemistry and Molecular Biology Department, University of the Basque Country (UPV/EHU), P.O. Box 644, E-48080 Bilbao, Spain.

* Corresponding author's email: llizmarzan@cicbiomagune.es

[#] These authors contributed equally.

EXPERIMENTAL DETAILS

Diffusion device design and fabrication

Custom diffusion devices were designed with Autodesk Inventor Software (Autosdesk Inc. Ca, USA) and fabricated using an Ultimaker 2 printer. The devices were printed with black Polylactic acid (PLA) with 90% filling density, employing a 0.4 mm Print Core AA nozzle (9529, Ultimaker) heated to 210 ºC prior to cell culture, PLA devices were rinsed with distilled water, dried, and sterilized with UV light. Biocompatible adhesive (H00191, Proclinic) was employed to bind the devices to the cover glass substrate with the scaffold attached.

Lentiviral transduction

Lentiviral particles were employed for long-term expression of eGFP and hygromycin resistance (656-4, pLenti CMV GFP Hygro, addgene). Cells were seeded in 2D and allowed to adhere overnight. After 24 h, 10 viral particles per cell (MOI 10) were added to the media. The following day, cells were positively selected with hygromycin B at a concentration of 100 µg/mL (0687010, Invitrogen). Cellular toxicity of lentiviral particles was determined by trypan blue staining. Transduction efficiency of more than 90% was confirmed by fluorescence microscopy at different days post-infection and by flow cytometry.

3D cell culture

Dissociated 3D cell cultures were prepared from the cell line MCF7 (ATCC#® HTB-22™) Adhered cells growing on a T-75 flask were trypsinized with 0.1% Trypsin-EDTA solution 1X (10779413, Thermofisher) and incubated for 3 minutes after rinsing with PBS solution. Once detached, the cells were suspended in plating media. Plating media was Gibco Dulbecco's Modified Eagle Medium (DMEM) (11520556, ThermoFisher) with 10% (v/v) of fetal bovine serum (FBS, 11573397, Thermofisher) and 1% (v/v) of Penicillin- Streptomycin (PenStrep, 11548876, Thermofisher). For counting, 10 µL of cell suspension was mixed with 10 µL of Trypan Blue and dispensed in a Cell Counting Chamber Slide (C10228, ThermoFisher) for automated cell

counting. Cell solution was centrifuged for 5 minutes at 850g, resuspended at 1000 cells/µL with plating media, and mixed 1:1 with Matrigel (356237, Corning™). The Matrigel-cell solution mixture was kept in ice and the pipette tips pre-chilled to avoid polymerization. 70 µL of the hydrogel-cell solution was then dispensed in the central chamber containing the scaffold and immediately incubated for 2 h at 37 ºC to promote gelation. After polymerization, plating media was added on top, in the media well, for nourishing the 3D culture.

Compound application

Methylene Blue (MB) (> 95% 28514, Sigma-Aldrich) was selected to assess the diffusion of compounds in the 3D cell culture model. Final concentrations of MB ranged from 1 µM to 20 µM in cell media. Cells were incubated 24 h prior to treatment with complete plating media. For XY diffusion assessment, 10x the final concentration of pre-irradiated MB was added to the lateral reservoir. For studying the diffusion in Z, pre-irradiated MB was applied on top of the 3D culture, in the media well. Irradiation of MB solution was performed for one hour with a light-emitting diode (LED) array with an emission wavelength of 640 nm and an energy density of 3.5 mW. To visualize the cytotoxicity gradient effect by confocal imaging, MB was applied to the lateral reservoir, incubated at 37 ºC for 2 h, and rinsed twice with media. Then, the media well was filled, and the entire device was irradiated for 1 h. Control experiments with non-exposed MB or without MB were conducted to confirm the specific effect of irradiated MB.

3D Cytotoxicity assessment

The cytotoxicity effect of MB was analyzed 24 h after treatment by several approaches. First, the media in the device was replaced for complete plating media with (1:100) of propidium iodide (PI), for staining of dead cells. The PI solution was incubated for 2 h prior to imaging assessment. Once imaging was completed, the hydrogel was depolymerized, and cell aggregates were retrieved to perform additional quantitative cytotoxicity tests. Thus, cell media was rinsed with PBS solution and the media well filled with 300 µL of cell recovery solution (354253, Corning). The device with cell recovery solution was incubated for 20 minutes at 4 ºC and complete depolymerization of Matrigel was promoted by pipetting carefully up and down. The solution was then pipetted into an Eppendorf tube and the device rinsed with PBS to recover all remaining cells. Subsequently, recovered cells were counted using a Neubauer cell chamber and divided for flow cytometry analysis and cell viability assay.

Flow cytometry

Cell viability after MB application was monitored using the FACSCanto II flow cytometer and FACSDiva 6.0 software (BD Bioscience). Collected cell solution expressing eGFP and stained with PI was centrifuged (5 min, 3500 rpm) and resuspended in 200 µL of PBS. A minimum of 5000 cells was analyzed. Illumination was performed with a 20-mW 488-nm argon-ion laser. Viable cells labeled with GFP were detected with a 530/30 filter and non-viable cells stained with PI with a 575/26 filter. The cell solution was also measured by flow cytometry for assessment of MB cell uptake, using a 695/40 filter. Posterior analysis was performed with Flow Jo v10.7.

Cell viability assay

Quantification of viable cells in the 3D culture was performed using the CellTiter-Glo (CTG) 3D Cell Viability Assay kit (354253, Corning). Collected cell culture after hydrogel depolymerization was centrifuged (5min at 775g), resuspended in PBS, and dispensed in 96 opaque-well plates. Each well containing 50 µL of cell solution was mixed with 50 µL of CellTiter-Glo 3D reagent and incubated at RT for 30 minutes. The solution of each well was vigorously mixed by pipetting up and down and incubated for 30 minutes more. Luminescence was measured with an Orion II LB 965 Microplate Luminometer (Berthold Technologies GmbH), using an integration time of 1 second per well.

Imaging of 3D cell cultures

Morphological analysis and imaging of 3D cell cultures were performed after 3-4 DIV. Images were acquired with a confocal microscope Zeiss LSM 880 (using ZEN software). For monitoring the spatial cytotoxic effect of MB, large images of the whole scaffold dimension (5.5x5.5 mm^2) and approximately 400 µm thickness were acquired with 10x objectives. For a more detailed analysis of cell aggregates, 20x and 40x magnifications were employed. After acquisition,

images were processed with ZEN software (ZEN 3.4 (blue edition), ZEISS) and exported by individual channels. Average Z-stack projections were imported to ScanR analysis® software (Olympus) for automated cell quantification. Signal intensity threshold and size filters were applied for image segmentation. TIBCO Spotfire® software (Perkin Elmer) was used to plot the X/Y position of the segmented cells.

Ink preparation and 3D printing of scaffolds

Nanocomposite inks were prepared by mixing 1 mL of a 20% wt. aqueous solution of gelatin with 40 mg of alginate and 1 mL of a gold nanorod (AuNR) solution with a concentration of 2 mM in gold. The samples were thoroughly mixed using a Thinky Mixer at 3500 rpm for 1 min. AuNRs were prepared followed a previously reported procedure.[1] AuNRs were washed prior to their incorporation to the ink formulation to remove excess CTAB, as previously described. 3D printed scaffolds[2] were prepared using a RegenHU 3D Discovery Bioprinter at room temperature using a pneumatic pressure driven cartridge with a 0.2 mm diameter needle, at a pressure of 0.2 MPa. After printing, the scaffolds were immersed in a calcium chloride bath for a few minutes.

Scaffold characterization

The rheological properties of the inks were characterized using a Physica MCR 302 rheometer (Anton Paar, Spain). All tests were carried out in triplicate at room temperature using a 25 mm parallel plate geometry and a solvent trap to prevent water evaporation. Frequency sweeps were carried out from 0.1 to 500 rad/s at 0.1% strain, determined by previously performed amplitude sweep assays, with a gap of 1 mm. Flow curves were also obtained for shear rates from 0.01 to 1500 s^{-1}. Finally, oscillatory-rotational-oscillatory tests were performed by applying a shear rate of 10 s^{-1} and studying the recovery of the inks at rest. The microstructure of the scaffolds was analyzed using a JEOL JSM-6490LV scanning electron microscope (SEM), operating at an acceleration voltage of 15 kV and at a working distance of 15 mm.

The stability of the scaffolds in cell culture media (cDMEM) at 37 ºC was assessed after recording the swelling of the material by a general gravimetry method at selected time intervals. The swollen hydrogels were removed, the excess of liquid absorbed with filter paper and the scaffold weighed. The swelling ratio (SR) was calculated using Equation 1:

$$SR = (W_s - W_d)/W_d \cdot 100 \quad (1)$$

where W_s is the weight of the swollen sample and W_d is the weight of the dried hydrogel sample.

SERS measurements

Two different Raman microscopes were employed for the different experiments, according to the required spatial resolution. To image large areas with low resolution (scanning step size 100 µm in X and Y axis), SERS spectra were acquired with a InVia Reflex Raman microscope (Renishaw plc) comprising an optical microscope (Leica) with a XYZ scanning stage coupled to a high-throughput Raman spectrometer equipped with a 1024x512 front-illuminated CCD detector and a grating of 1200 grooves/mm, using a line-shaped 785 nm laser excitation source (maximum 119.50 mW), and recording in static mode at standard confocality through a 10x objective (numerical aperture N.A. = 0.5) with 1s integration time (or 0.1 s for large diffusion gradients), at 15.15 mW laser power. SERS images were then generated after cosmic ray removal and baseline subtraction (intelligent fitting procedure) by plotting the signal intensity of MB around 450 cm^{-1} as a function of the X and Y position using the tools implemented in the Wire 4.4 software package and JupyerNotebook. To image areas with higher resolution (scanning step size 16 µm or less) and 3D imaging, SERS maps were recorded with a high-resolution confocal Raman microscope alpha 300R (Witec GmbH) comprising an optical microscope (Zeiss) with a motorized XY scanning stage and linked piezo scanner fiber-coupled to an ultra-high-throughput Raman spectrometer (UHTS400-NIR) equipped with a 1024x128 back-illuminated deep depleting CCD detector (DU401 BR-DD, Andor) and a 300 groves/mm grating. As excitation source, a 785 nm laser with tunable output power was used, and spectra were collected through 20x (N.A.=0.5) or 63x (N.A.=1) water immersion dip-in objectives, with 10 or 50 ms integration times at 7 mW laser power (if not otherwise stated). The XY scanning stage was used for all confocal SERS mappings except for the high-resolution XZ profile and Z-stack

maps for the 3D image in Figure S4, which were acquired using the piezo-scanner. SERS images were generated after cosmic ray removal and background subtraction (Shape) using the True Component Analysis tool available in the Project5/Project5+ software (Witec) packages. 3D SERS images were created by reconstruction of Z-stack images with ImageJ software. Images of time-dependent MB diffusion in Figure 3a were additionally smoothed applying a 5x5 Median filter.

PLGA-MB capsules

PLGA nanoparticles loaded with methylene blue were synthesized by a single emulsion solvent evaporation method.[3] Briefly, 50 mg of PLGA and 2 mg of MB were dissolved in dichloromethane (5 mL), and subsequently added to an aqueous solution of PVA (MW 9–19 kDa, 25 mL, 5% w/w). This mixture formed an emulsion under ultrasonic stirring at 75% amplitude for one minute in an ice bath (tip-sonicator Branson, Digital Sonifier). The emulsion was left under magnetic stirring to completely evaporate the organic solvent (4 h) at room temperature. Subsequently, the samples were purified by 3-fold centrifugation at 8000 rpm for 15 min at 4 °C and the pellets were redispersed in deionized water. Finally, they were kept at -20 °C until use. MB concentrations were quantified by UV-Vis spectroscopy using a calibration curve obtained with commercial MB solutions prepared in water. Nanoparticle size distributions and zeta potentials were measured using a zeta sizer Nano ZS (Malvern Instruments Ltd., Worcestershire, United Kingdom), for each sample by triplicate.

ROS species generation after MB irradiation:

The production of $^1O_2$ was measured after irradiation of a 20 μM MB solution, containing the dye 9,10-Anthracenediyl-bis(methylene)dimalonic acid (ABDA). ROS production was followed by a decrease in ABDA absorbance (at 380 nm), which occurred upon reacting the dye with the oxidant species. A stock solution of ABDA in DMSO (~10 mM) was subsequently used in the preparation of 0.4 mM ABDA in PBS. The experiments were carried out in 96 well-plates. ABDA solutions (100 μL) were then mixed with 100 μL of MB (40 μM), to a final concentration of 20 μM, and then irradiated for 60 min with an emission wavelength of 640 nm and an energy density of 3.5 mW for 60 min. The absorbance of ABDA was finally collected, comparing the results with those obtained without MB or without lamp irradiation.

References:

(1) Scarabelli, L.; Sánchez-Iglesias, A.; Pérez-Juste, J.; Liz-Marzán, L. M. A "tips ´n tricks" Practical Guide to the Synthesis of Gold Nanorods. *J. Phys. Chem. Lett.* **2015**, *6*, 4270-4279.

(2) García-Astrain, C.; Lenzi, E.; Jimenez de Aberasturi, D.; Henriksen-Lacey, M.; Binelli, M. R.; Liz-Marzán, L. M. 3D-Printed Biocompatible Scaffolds with Built-In Nanoplasmonic Sensors. *Adv. Funct. Mater.* **2020**, *30*, 2005407.

(3) Song, C. X.; Labhasetwar, V.; Murphy, H.; Qu, X.; Humphrey, W. R.; Shebuski, R. J.; Levy, R. J. Formulation and Characterization of Biodegradable Nanoparticles for Intravascular Local Drug Delivery. *J. Controlled Release* **1997**, *43*, 197–212.

SUPPLEMENTARY FIGURES

Section S1: SERS performance of gelatin-alginate 3D networks containing AuNRs (Figures S1-S4)

Section S2: Mechanical characterization of nanocomposite scaffolds and their biocompatibility (Figures S5-S7)

Section S3: Screening of MB diffusion with spatio-temporal resolution (Figures S8-S11)

Section S4: MB cytotoxicity in 3D cancer models (Figures S12-S14)

Section S1: SERS performance of gelatin-alginate 3D networks containing AuNRs

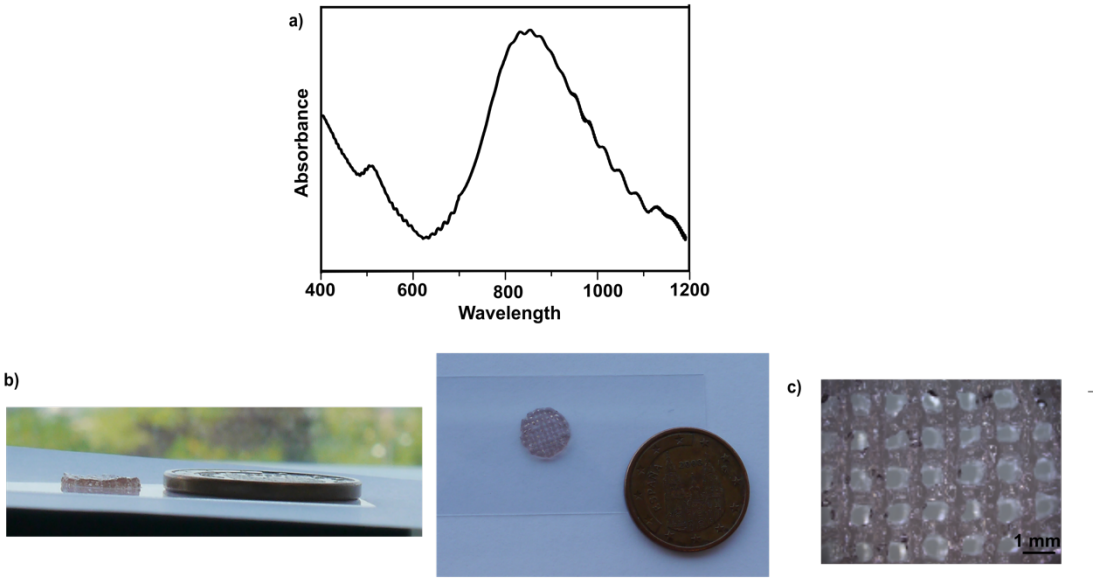

Figure S1. a) Vis-NIR spectrum of a gelatin/alginate (2%) ink containing 1 mM of AuNRs. b) Photographs of an illustrative nanocomposite scaffold from the side and from the front (a 5 €cent coin is incorporated in the picture for comparison). c) Higher magnification image of the scaffold obtained through a Greenough stereo microscope.

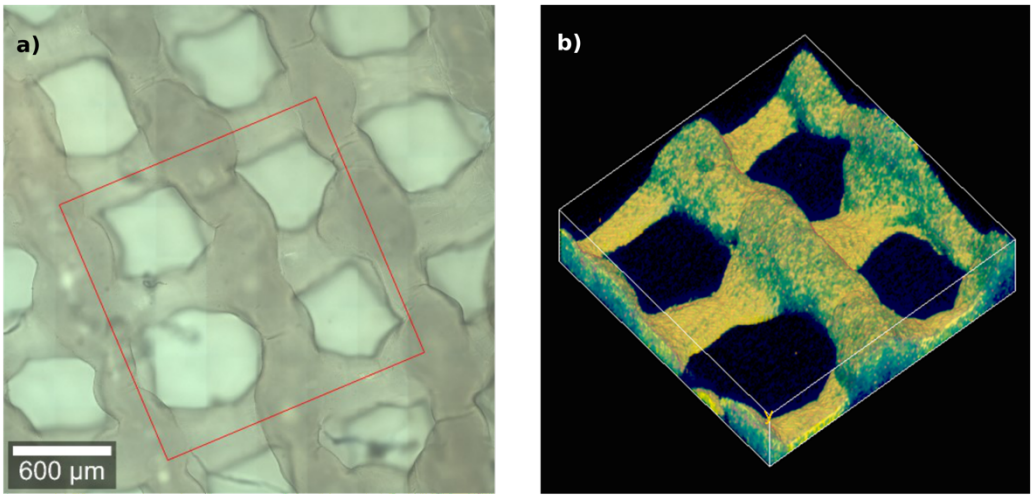

Figure S2. 3D projection of MB distribution along the scaffold after 24 hours of MB administration. The SERS signal of a 10 µM MB solution in cell media (DMEM, 10% FBS) was scanned within the area labeled by the red square in the left-hand optical microscope image. The measured cube presented the following dimensions in X, Y and Z: (1.5 x 1.5 x 0.5) mm^3. The SERS map in the right-hand panel was acquired by confocal Raman microscopy, with a 20x immersion objective and a spatial resolution of 10 µm in XY and 20 µm in Z. To visualize the 3D image, the different Z-stacks were reconstructed to produce a three-dimensional rendering.

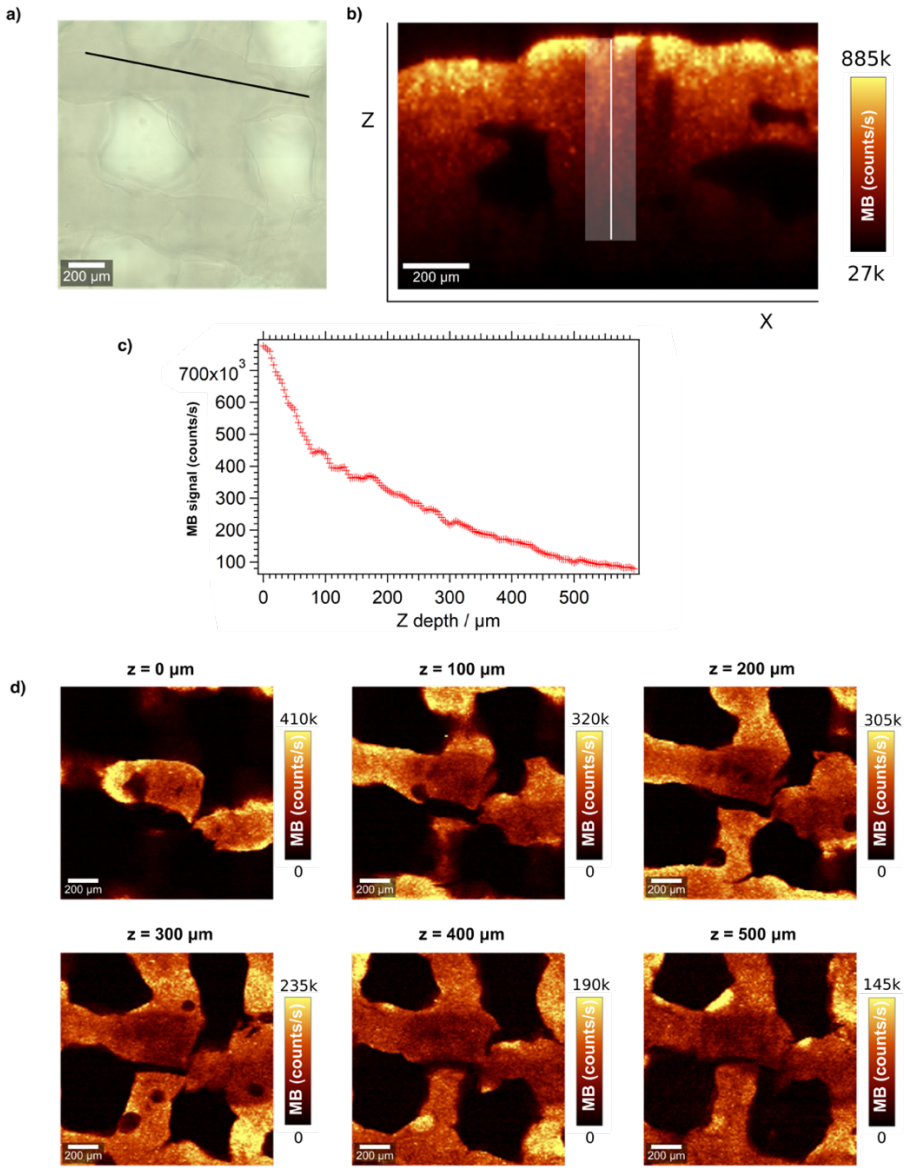

Figure S3. SERS signal decay of MB (10 µM) solution at deeper imaging planes along the Z-axis in gelatin-alginate (2%) scaffolds. The samples were immersed in water and covered with a coverslip (thickness #1) to maintain constant environmental conditions and to avoid dry-out during imaging. a) Bright-field (reflection) image of the scaffold. b) Confocal MB SERS profile down to 800 µm scaffold depth, recorded along a 1.26 mm line corresponding to the black line indicated in a), with a 785 nm excitation laser, power of 30 mW, integration time of 10 ms and using a 20x (NA=0.4) air objective. The scanning step size was set to 10 µm in XZ. Generally, the highest SERS intensity was observed close to the surface of the scaffold, thereby depicting its morphology. Large pores and holes within the scaffold below the surface could be also imaged. c) Cross section profile of the MB signal along Z (marked by the white line), and averaged over 150 µm along X (indicated by the shadowed area), showing a continuous decrease in SERS intensity with increasing depth. Small alterations of this behavior may be due to local structure inhomogeneities and/or to the presence of larger aggregates within the scanned area. d) MB SERS images recorded from different planes (depths) with an excitation at 785 nm, laser power of 30 mW, integration time of 10 ms and using a 20x (NA=0.4) air objective. Scanning step size was set to 10 µm in XYZ. The SERS signal was normalized for each image individually, showing the morphology and structure of the scaffold at different heights, down to a depth of 0.5 mm.

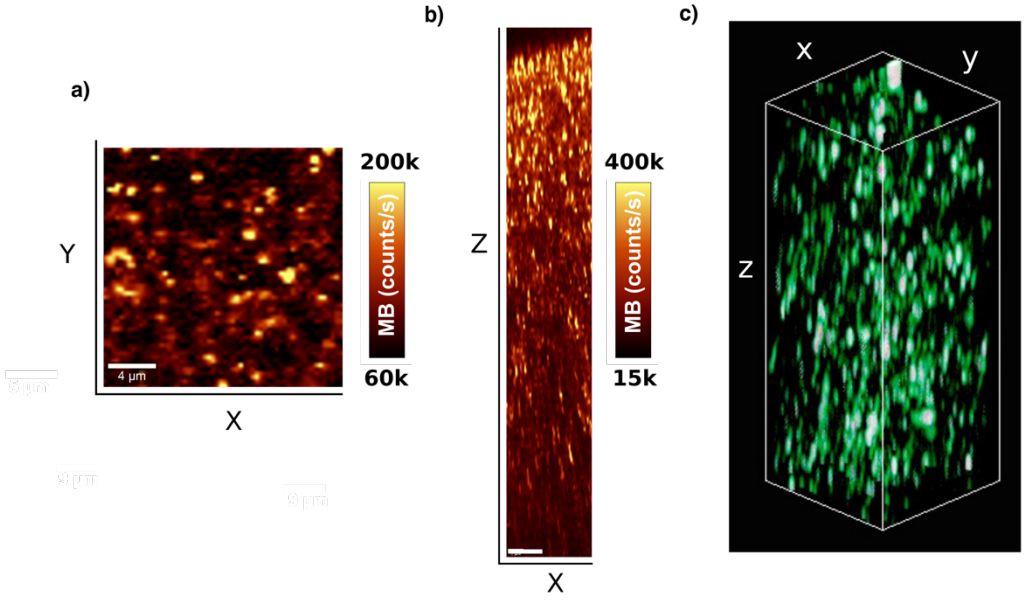

Figure S4. High-resolution SERS imaging of MB in XY-plane (a) and along Z-axis (profile map) (b), and (c) in 3D by reconstruction of XY images of a Z-stack at high magnification (63x water immersion objective, NA=1) recorded with a 785 nm laser. Image a) was measured with power of 10 mW, integration time of 10 ms and scanning step sizes of 0.33 μm in XY. The scale bar: 4 μm. Profile image b) was measured with power of 20 mW, integration time of 10 ms and scanning step sizes of 0.66 μm in X and 2 μm in Z. The MB signal was detected up to 300 μm below scaffold surface (Z-axis) Scale bar: 20 μm. Images for the reconstruction c) were recorded with power of 10 mW, integration time of 10 ms and with scanning step sizes of 0.333 μm in XY and 2 μm in Z. Dimension of the measured cube is (25 x 25 x 60) μm^3. The MB signal reflects the distribution and density of AuNR hotspots embedded in the scaffold, and available for sensing.

Section S2: Mechanical characterization of nanocomposite scaffolds and their biocompatibility (Figures S5-S7)

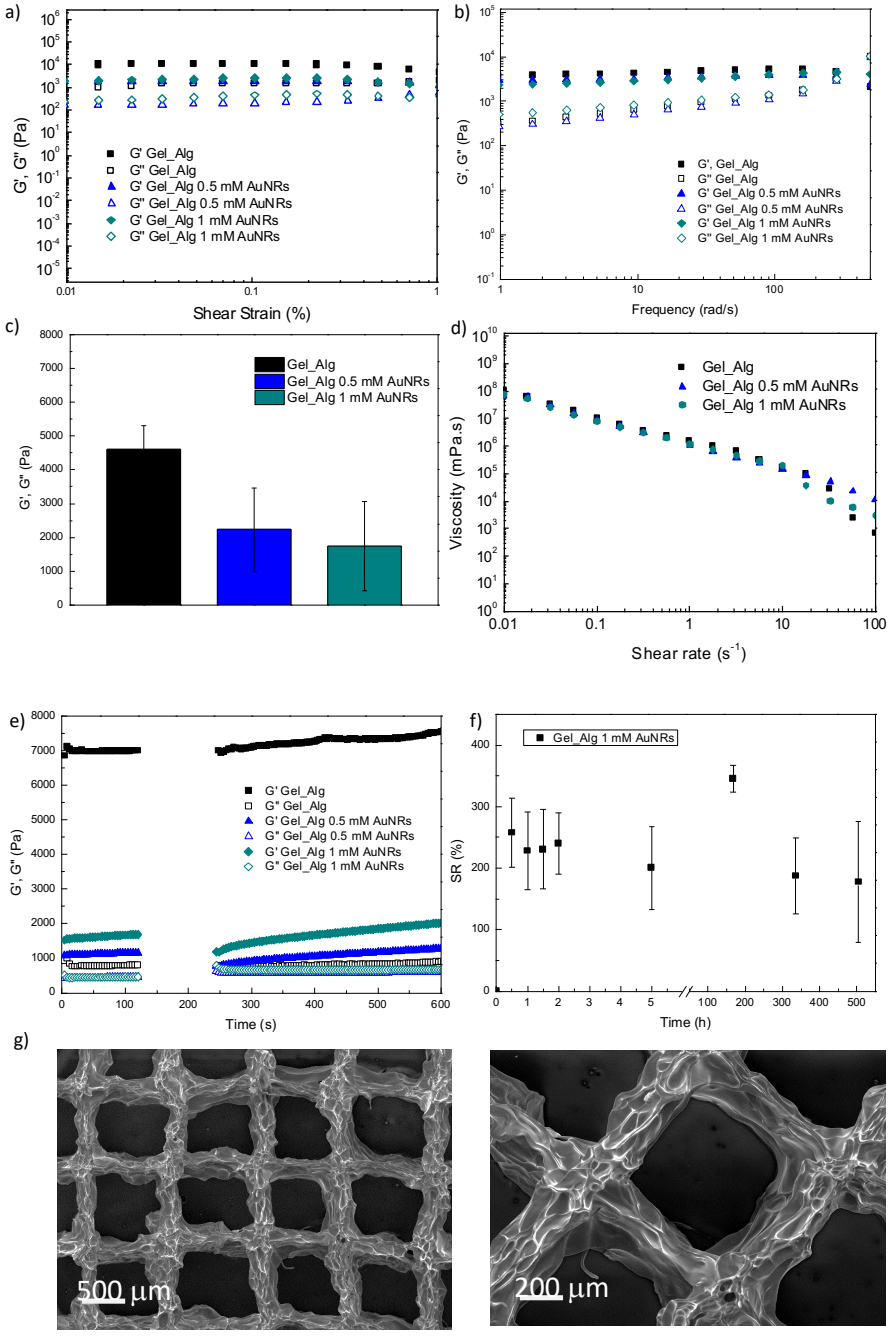

Figure S5. Rheological characterization of the hydrogels used as inks for 3D printing. a) Strain sweeps for gelatin (10%) and alginate (2%) with different AuNRs concentrations. b) Frequency sweeps at 0.1% strain. c) Storage moduli values at f = 1 Hz, for gelatin-alginate inks. The storage moduli of the inks were in the range of 2000 Pa and were reduced after addition of AuNRs, indicating that the particles disrupt the gel transition recovery of gelatin chains. d) Flow curves at different AuNRs concentrations, as labeled. e) Thixotropy tests show a quick recovery ability of the viscoelastic properties, thereby ensuring a good printing fidelity of the scaffolds with 75% recovery of the viscosity after a few seconds. f) Swelling studies of printed scaffolds during 20 days of incubation in cDMEM. g) SEM images of grid-like scaffolds with holes of ca. 700 µm.

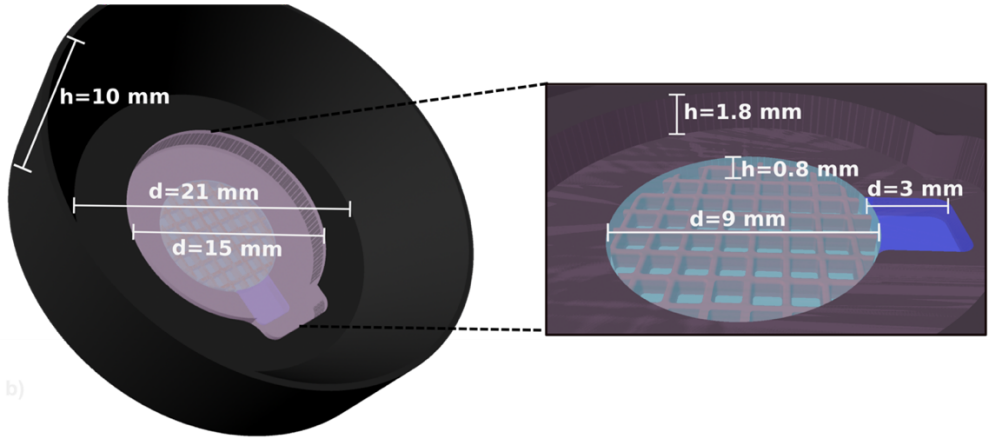

	Scaffold-hydrogel chamber	Compound reservoir	Media well	Immersion well
Area (mm^2)	63.6	9	176.6	346.18
Volume (µL)	50.88	7.2	318	1000

Figure S6. Dimensions of the cell culture device. Illustrations of the custom cell culture device designed with AutoCAD software (Illustrator) indicating the main dimensions. Summarized in the table are the area and volumes of the various compartments. The 3D culture had a thickness of 0.8 mm and was nourished with a minimum of 300 µL of media. Additional media could be poured to fill the whole device and perform SERS measurements with immersion objectives. The device also supported the addition of the compound in a controlled compartment to study its diffusion through the 3D culture.

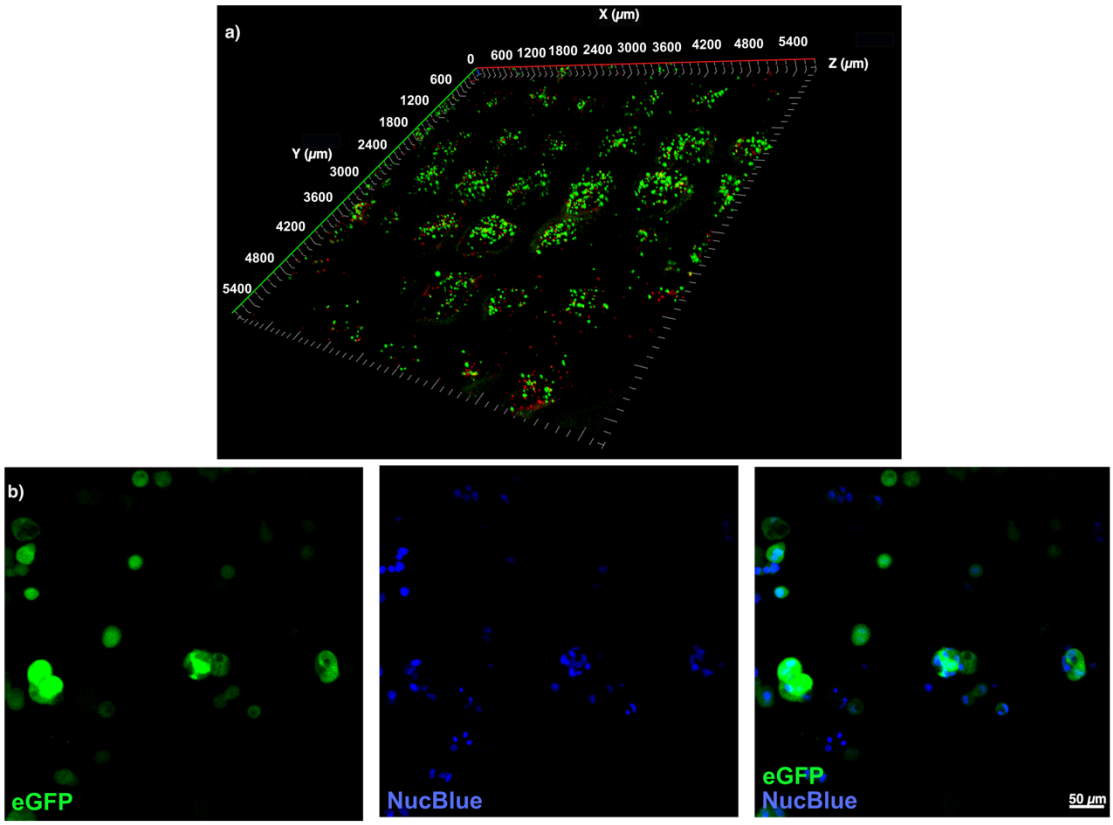

Figure S7. Characterization of (a) the 3D cell culture by confocal imaging. a) Example of reconstructed live images employed to monitor the distribution of live cells after addition of MB. MCF7 cells expressed eGFP; dead cells were labeled with PI 24 h after application of MB solution. For automated quantification of viable cells in the 3D system, a volume of 5.5x5.5x0.4 mm_3 was imaged. b) (MCF-7) 3D cell aggregates embedded in Matrigel were formed (in 3D) after 3-4DIV (within) around the nanocomposite scaffold. (MCF-7 cells with eGFP were labeled with NucBlue for visualization of individual nuclei.) MCF-7 cells expressing eGFP were labeled with NucBlue to visualize individual nuclei.

Section S3: Screening of MB diffusion with spatio-temporal resolution (Figures S8-S11)

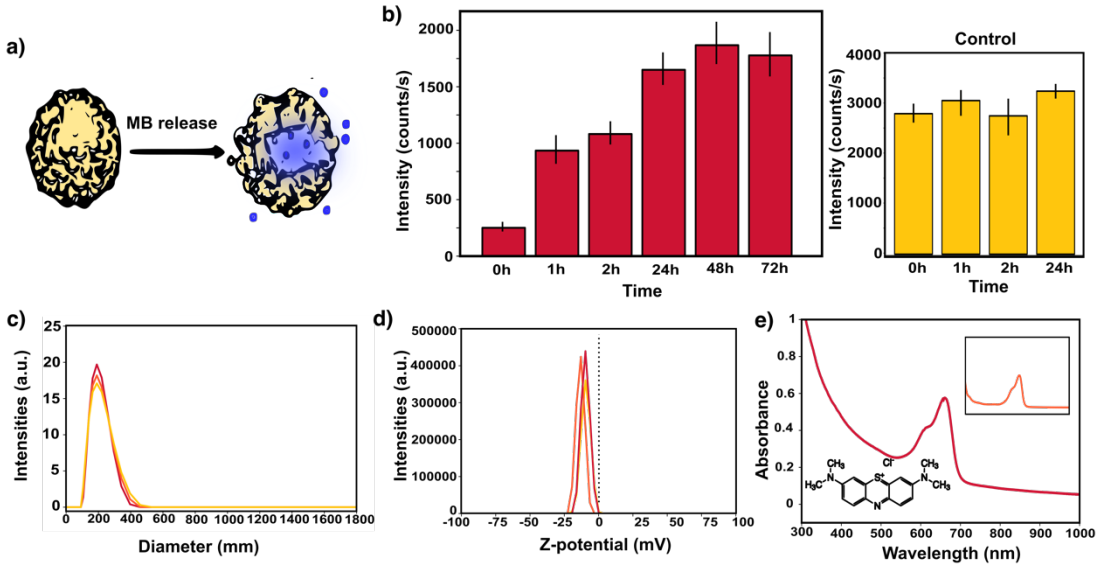

Figure S8. a) PLGA capsules with a 50:50 lactic/glycolic content ratio (pale yellow spheres), containing MB (blue dots). Schematic representation illustrating the gradual release of Methylene Blue (MB) to the extracellular media, owing to spontaneous degradation of the polymeric capsules. By incubation of such capsules within the nanocomposite scaffolds, we could efficiently monitor MB delivery via SERS measurements. b) Registered SERS intensities at 450 cm^{-1}, at successive times upon PLGA-MB capsules incubation with the plasmonic scaffold. The gradual increase in SERS signal accounted for the release of MB into the extracellular media. In contrast, scaffolds under control conditions (yellow bars), in which 50 μM of free MB was administrated, provided a homogenous SERS signal over time. Each data point corresponds to the average signal from 20 collected points, for two independent experiments. c) Particle size distribution of MB-PLGA capsules determined by DLS in Milli-Q water, as intensity distribution. Mean hydrodynamic diameters= 204 ± 3 nm. (d) Zeta-potential distribution I(ζ) of MB-PLGA capsules, measured in Milli-Q water. ζ = -9.5 ± 0.2 mV. Results are shown for 3 different measurements. e) UV-Vis-NIR spectrum of MB contained inside PLGA capsules, the inset displays the UV-Vis-NIR spectrum of free MB, released from the capsules after 24 hours. In this case, to separate the capsules from free MB, a centrifugation step was performed.

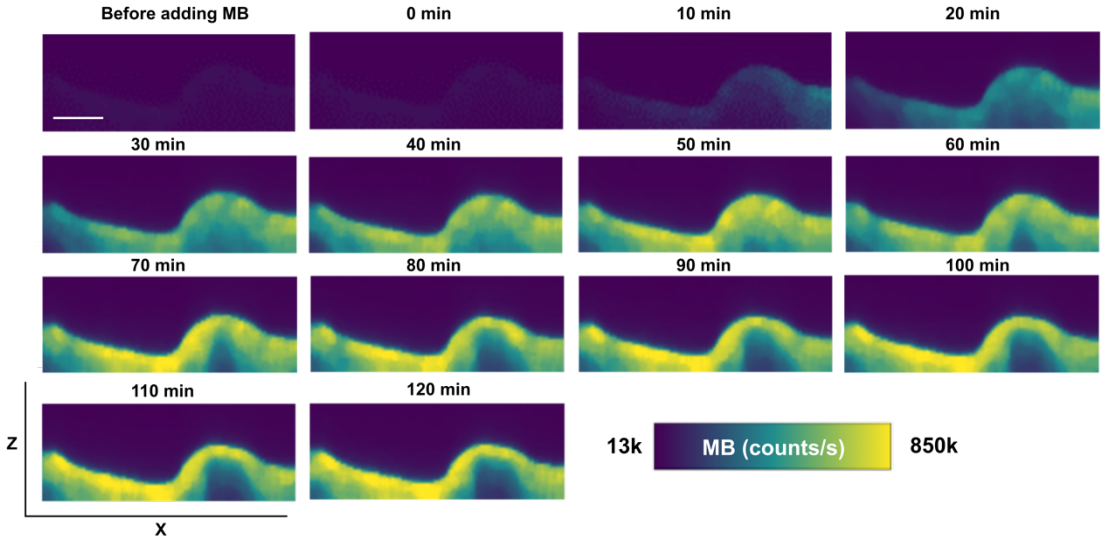

Figure S9. Time-resolved mapping of the MB-SERS signal in the XZ plane (profile). MB (10 μM) was delivered to the scaffold at the compound reservoir incubated in Mili-Q water. SERS profiles were measured at laser excitation of 785 nm with a power of 15 mW, integration time of 10 ms and a scanning step size of 10 μm, using a 20x air objective (NA=0.4). The intensity corresponds to the signal of the whole MB fingerprint. To smooth the images, a 5x5 Median filter was applied after cosmic ray removal, background subtraction and true component analysis. The images reveal no significant intensity changes at the surface after 90 min, indicating saturation (equilibrium).

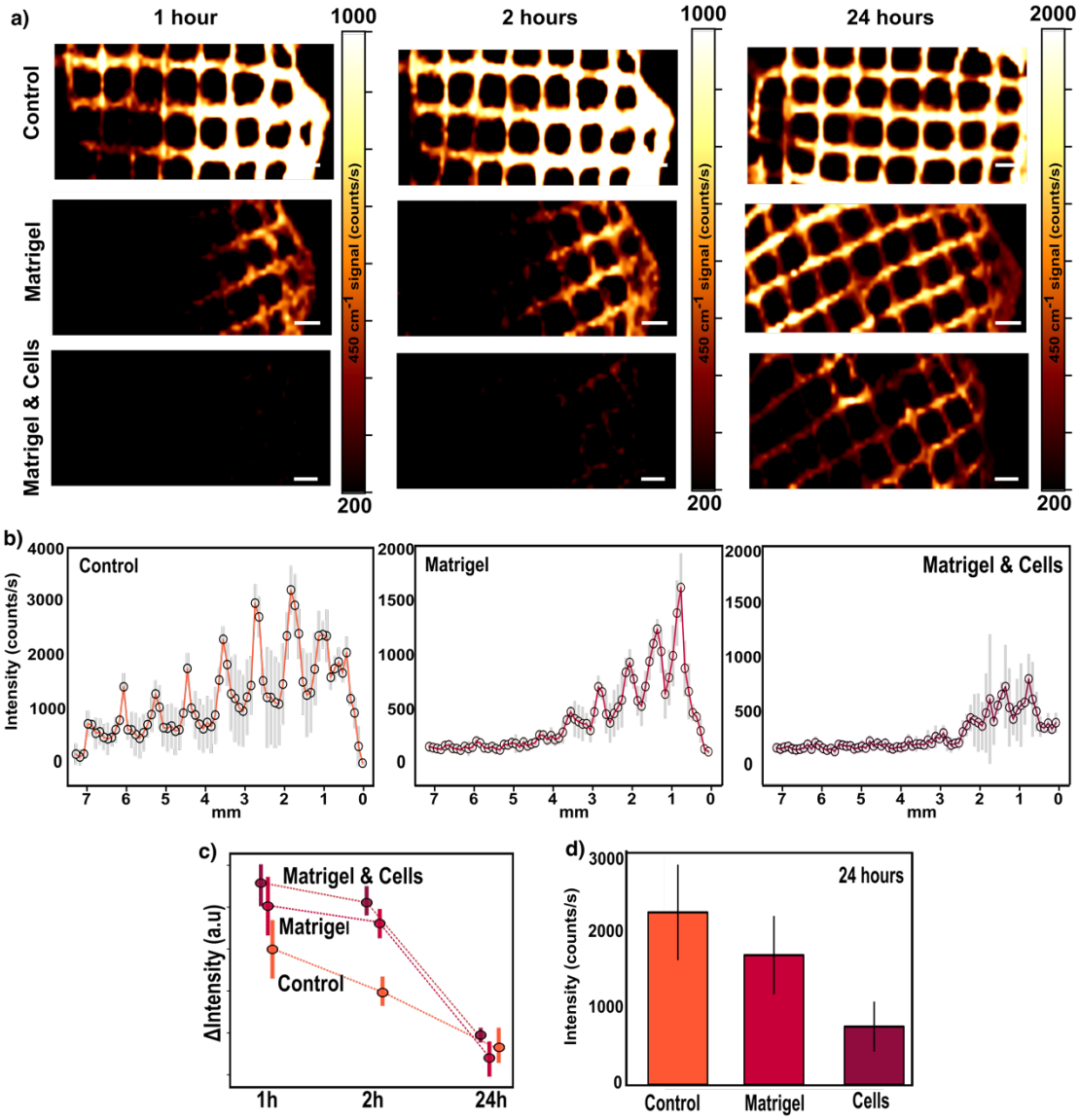

Figure S10. a) Additional SERS mappings, displaying the profiles of MB distribution along X and Y axes within nanocomposite scaffolds, at successive times and under different conditions: pristine scaffolds, scaffolds embedded in Matrigel, and cells embedded in Matrigel loaded with high cell density ($2x10^6$ cells/mL). Scale bars are 600 μm b) The SERS intensity at 450 cm^{-1} of illustrative experiments is plotted, showing the diffusion profiles along the X-axis. Each point represents the average and the standard deviation obtained from SERS intensities along the Y-axis. The step size is 100 μm. c) Plot comparing the differences in SERS intensity between one area of the scaffold, selected as that closest to the compound reservoir with the highest SERS intensity, and another located at 3000 μm away in the X-axis from the first one. The SERS intensities were normalized for every experiment and then this parameter was calculated, by subtracting SERS intensities, at different times and conditions. Each point denotes the average value from three independent experiments. d) Average of the SERS intensity at 450 cm^{-1} after 24 hours of MB administration (10 μM) from the compound reservoir, once equilibrium was reached (homogenous distribution of MB along X and Y axes). Each data point corresponds to the average signal from 200 collected points within two independent experiments (n = 200, N = 2). For all measurements, an excitation laser line at 785 nm through a 10x objective, with a power of 15.15 mW for 0.1 s, was used.

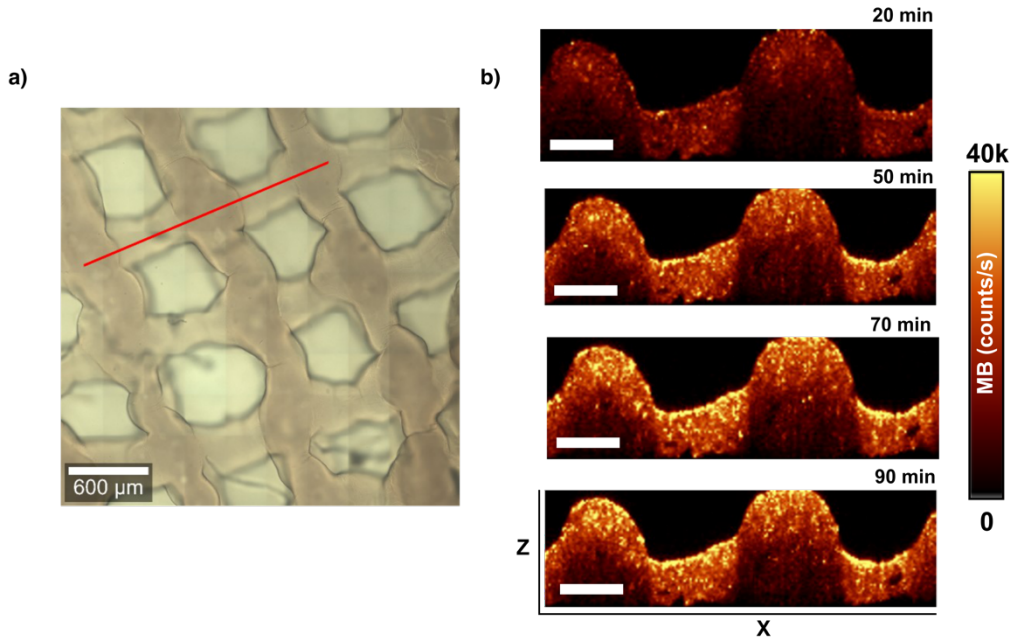

Figure S11. Scanning SERS intensity maps at 450 cm^{-1} along the X and Z axes of the nanocomposite scaffold, at the region labeled with the red line in the left image. SERS mappings were registered through successive times (0, 20, 40, 50, 70, 90 min) upon MB (10 μM) administration from the top media well. SERS signals were recorded with a 785 nm excitation laser through a 20x immersion objective in confocal mode, with a power of 7 mW, 50 ms of integration time, and a step size of 10 μm. Scale bars: 200 μm.

Section S4: MB cytotoxicity in 3D cancer models (Figures S12-S14)

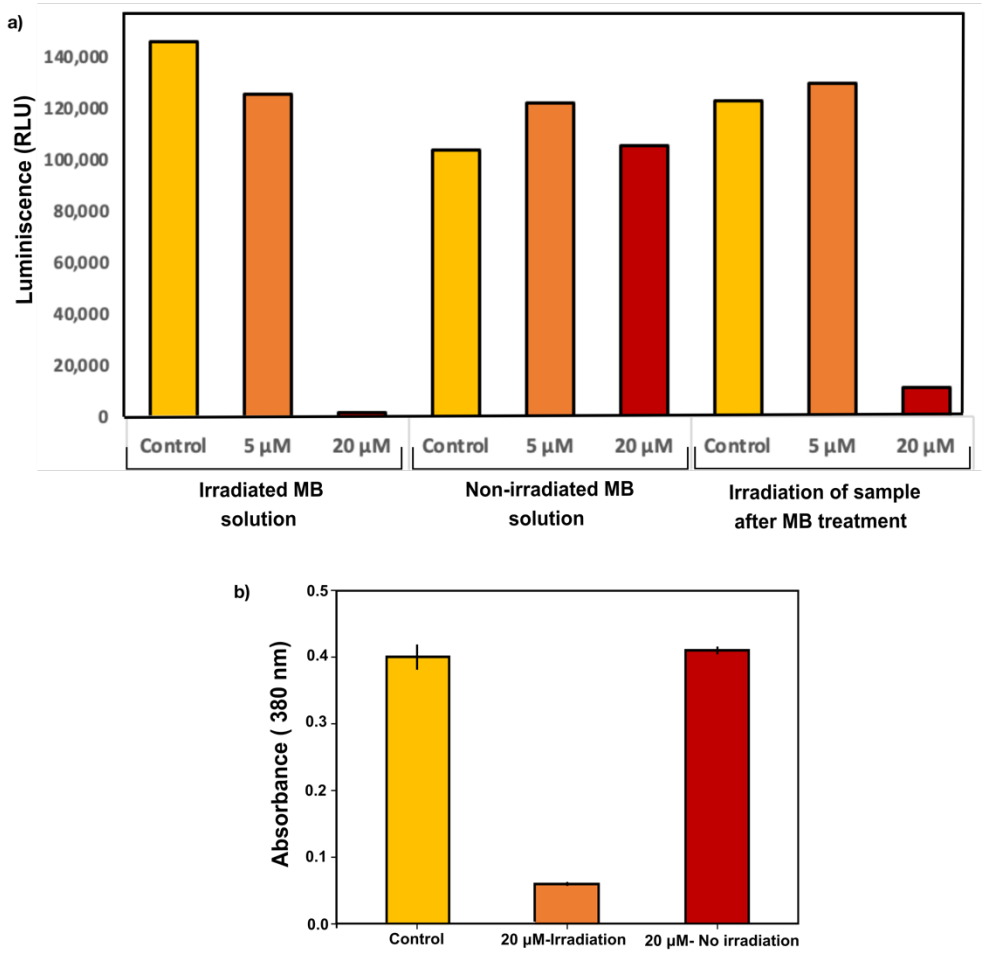

Figure S12. a) Luminescence output 24h after MB challenging at two different concentrations (5 µM and 20 µM), with or without red-lamp irradiation for 1 hour. We compared the effects of MB on cell viability when the light photoactivation step occurred before or after drug delivery to the cell culture. Non-irradiated MB had a negligible impact on cell viability at this concentration range, offering similar values of luminescence to those obtained for control conditions. On the contrary, 20 µM of irradiated MB exhibited an intense cytotoxicity in both photoactivation procedures, owing to the generation of oxidizing species. b) ROS generation by MB (20 µM) after 60 min of red lamp illumination (640 nm). The production of ROS acts by reducing ABDA molecules, present in the solution at 0.2 mM, which eventually leads to a decay in the absorbance at 400 nm.

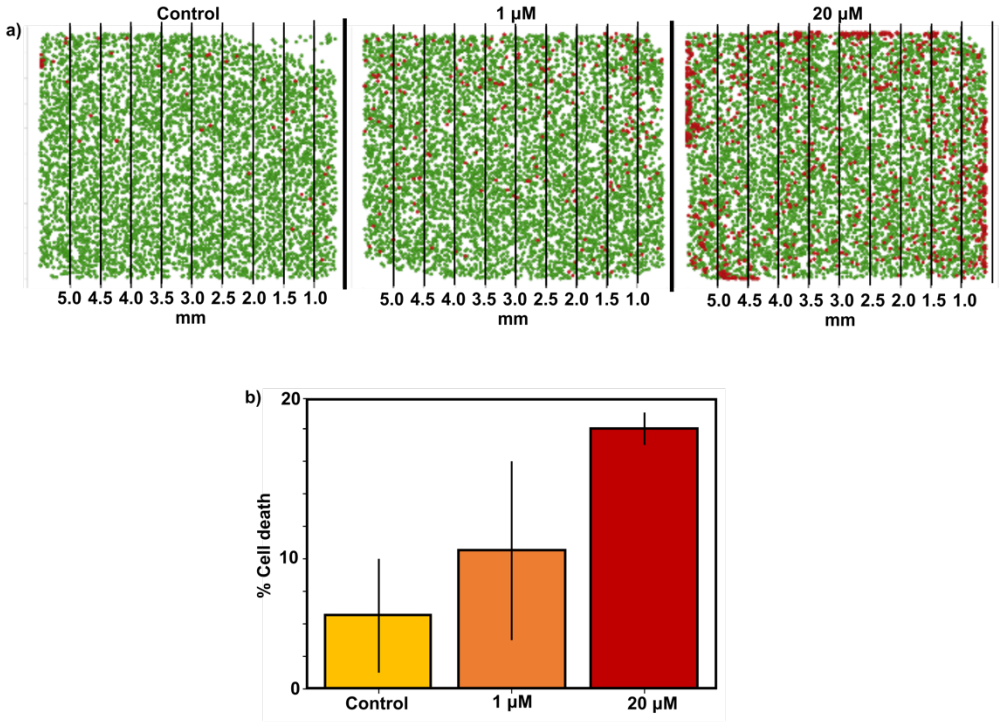

Figure S13. a) Quantification of cell viability (%) under control conditions, 1 µM, 20 µM of MB after 24 hours of MB administration at the compound reservoir; MB was previously activated by red lamp illumination for 60 min. The acquired 3D images for each condition were computationally segmented in columns separated by 0.5 mm. The obtained results did not display a well-defined gradient of cell death along the X-axis. The red points label the PI positive cells (dead cells), whereas those colored in green indicate cells expressing GPF (live cells). b) Ratio of PI positive cells to the total cell population at different MB concentrations.

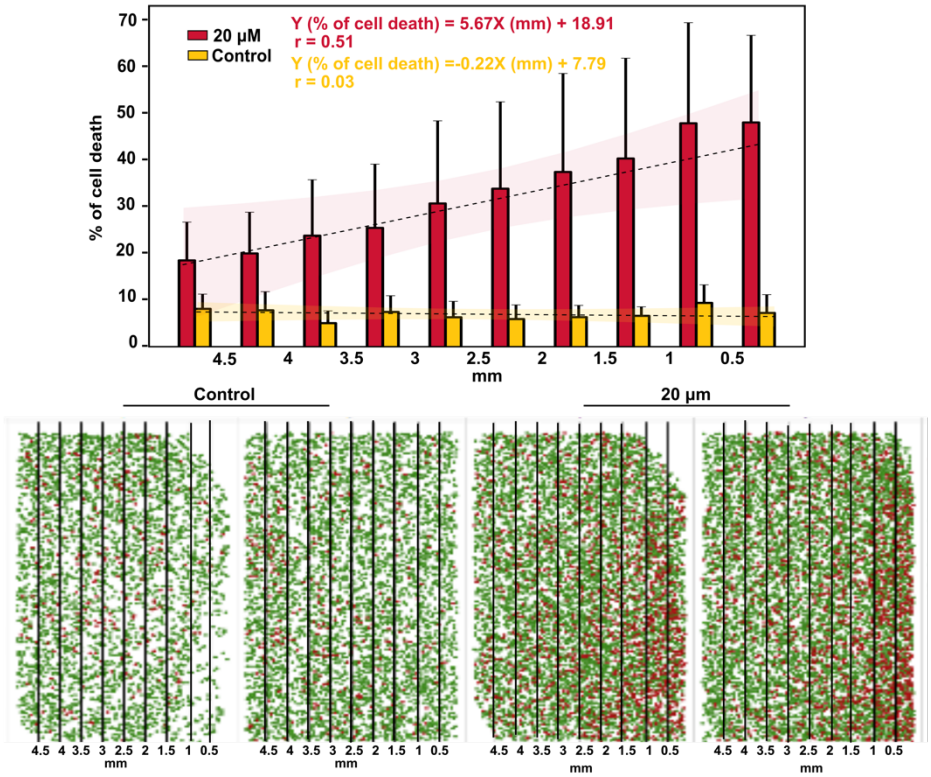

Figure S14. Quantification of cell viability (%) under control conditions and with 20 µM of MB delivered by means of the following approach. Cells were challenged with MB, applied at the lateral reservoir for 2 hours. Then cell media containing the diffusing compound was replaced. To better visualize the impact of this procedure on cell viability, 3D images from each sample were computationally segmented in columns separated by 0.5 mm. Error bars show the standard deviation of four independent cell assays, including two samples with and two samples without scaffold. The yellow and purple bars are linear fits showing the correlation of cell cytotoxicity (%) with the distance (mm) in control and 20 µM of MB, respectively. Both include a regression line (dotted line) and 95% confidence interval. In addition, the corresponding Pearson correlation coefficient (r) between the two variables is indicated in the inset. The images in the lower panels display the automated quantification of cell viability percentage from illustrative control and 20 µM samples without scaffolds. Lines indicate columns into which the images were divided to study the distribution of PI (red) and GFP signals (green).